International Journal of Medical Physics, Clinical Engineering and Radiation Oncology, 2025, 14(2), 15-32
https://www.scirp.org/journal/ijmpcero
ISSN Online: 2168-5444
ISSN Print: 2168-5436

Patient-Specific QA Using Multidimensional Detectors in Single Isocenter Multitarget Stereotactic Radiotherapy for Multiple Brain Metastasis

Miyu Ishizawa[1], Yuya Miyasaka[1], Hongbo Chai[1], Hikaru Souda[1], Mayumi Ichikawa[1], Hiraku Sato[2], Takeo Iwai[1]

[1]Department of Heavy Particle Medical Science, Yamagata University Graduate School of Medical Science, Yamagata, Japan
[2]Department of Radiology, Faculty of Medicine, Yamagata University, Yamagata, Japan
Email: miyu.ishizawa.r1@gmail.com

How to cite this paper: Ishizawa, M., Miyasaka, Y., Chai, H., Souda, H., Ichikawa, M., Sato, H. and Iwai, T. (2025) Patient-Specific QA Using Multidimensional Detectors in Single Isocenter Multitarget Stereotactic Radiotherapy for Multiple Brain Metastasis. *International Journal of Medical Physics, Clinical Engineering and Radiation Oncology*, **14**, 15-32.
https://doi.org/10.4236/ijmpcero.2025.142002

Received: February 11, 2025
Accepted: March 29, 2025
Published: April 1, 2025

Abstract

Purpose: This study used ArcCHECK (AC) to investigate the connection between target- and treatment plan-dependent parameters and the gamma passing rate (GPR) to determine the characteristics of patient-specific quality assurance (PSQA) in single isocenter multitarget (SIMT) stereotactic radiotherapy (SRT). **Methods:** Twenty-four SIMT SRT treatment plans (92 targets) were evaluated. All treatment plans were developed using dynamic conformal arc therapy (DCAT), and the equivalent multi-leaf collimator (MLC) field size, distance from the isocenter (IC), and monitor/Gy were determined. The absolute dose error from the treatment planning system (TPS) was calculated using 92 targets and an ionization chamber detector. Gamma analysis was performed with AC, a multidimensional detector, and SNC patient software. Threshold values of 10% and 20%, absolute and relative dosimetry, global mode, and dose difference (DD)/distance-to-agreement (DTA) criteria of 3%/2 mm, 2%/2 mm, 2%/1 mm, and 1%/1 mm were employed. Differences in GPR were assessed for each condition. The correlation of GPR with treatment planning parameters and ionization chamber detector errors was investigated. **Results:** With stricter DD (2%/2 - 2%/1 mm), the GPR fell by an average of 18.6% (86.4% - 67.8%). The average equivalent MLC field size was moderately correlated with GPR and weakly correlated with the maximum error of the ionization chamber detector and MU/Gy, but not with the max target-IC distance. In the case of small targets, the dose in the center was relatively acceptable, but the lower dose range outside of the target was less responsive, fre-

quently resulting in failures. **Conclusions:** In SIMT SRT, we investigated in detail the differences in GPR based on the AC's gamma analysis conditions, as well as the relationship between the GPR and treatment planning parameters. The GPR was found to be significantly reduced when the average equivalent MLC field size was small, *i.e.*, there were many small target sizes.

Keywords

Single Isocenter Multitarget, Dynamic Conformal Arc, Brain Metastasis, Patient-Specific Quality Assurance

1. Introduction

Radiotherapy for patients with multiple brain metastases has shifted from whole-brain irradiation to stereotactic radiotherapy (SRT), with single isocenter multi-target (SIMT) SRT irradiation becoming more popular recently [1]. This has been shown to provide excellent local control while minimizing neurocognitive decline [2] [3]. Furthermore, treating multiple targets of SIMT simultaneously can significantly reduce treatment time when compared to irradiating each target separately [4]. Reducing treatment time can improve patient comfort, compliance, efficiency, and clinic workflow [5]-[7].

SIMT for intracranial targets typically results in a steep dose gradient around multiple and small targets, with no target at the isocenter (IC). Therefore, even minor misalignments can significantly alter the dose entering the target, resulting in unacceptable errors and undesirable clinical outcomes [5] [8]. Hence, it is strongly advised to conduct patient-specific quality assurance (PSQA) before treatment [9]-[11]. However, accurate dosimetry is difficult due to lateral electronic disequilibrium, under-sampling, and volume-averaging effects caused by detectors with volumes close to the irradiation field due to the target's small size, and difficulty in detector [10] [12] [13]. Furthermore, multiple off-axis lesions must be measured because the target is not at the IC [5] [14]. Therefore, there are more challenges than with PSQA when using common irradiation methods like intensity-modulated radiation therapy (IMRT) and volumetric-modulated arc therapy (VMAT).

There are currently several devices available for PSQA of SIMT SRT, including low and high detector-density ionization chamber/diode arrays [15]-[20], small-volume ionization chamber/diamond detectors [21], films [21], radiochromic gel dosimeters [22], electronic portal imaging devices [23], machine delivery log files [24] [25], and polymer gels [26]. Each of the tools mentioned above has both advantages and disadvantages. Recently, there is also a Monte Carlo independent calculation system specialized for SIMT [27] [28].

Leon *et al.* used five commonly available PSQA tools: Sun Nuclear ArcCHECK (AC) [17] and SRS MapCHECK [15] [16], GafChromic EBT Radiochromic Film [21], machine log files [24] [25], and Varian Portal Dosimetry [11]. The sensitivity to various multi-leaf collimator (MLC) and dose-related errors, as well as the cri-

teria for gamma analysis for correctly detecting them, were investigated in conjunction with clinical objectives. They propose evaluating SIMT PSQA results separately based on the size of the PTV and its distance from the IC. To the best of our knowledge, only a few papers have thoroughly evaluated the characteristics of AC in terms of parameters such as PTV size and distance from the IC in SIMT. Therefore, we investigated the relationship between the PSQA's gamma pass rate (GPR) and parameters related to treatment planning to better understand the characteristics of AC in SIMT.

2. Material and Methods

2.1. Patients Selection

Twenty-four plans for at least two intracranial lesions treated with SIMT SRT at our hospital were retrospectively selected. The study cohort consisted of 73 cases that completed treatment within the period approved by the ethics review committee. To assess the effects in cases where the target was not located at the isocenter, single-target cases (49 cases) were excluded from the analysis. As a result, 24 cases were registered, and there were 92 irradiated targets. All PTVs received at least 27 Gy. The target volume sizes varied from 0.1 cm^3 to 9.9 cm^3 with a median of 0.8 cm^3. The number of targets varied from 2 to 11 (Table 1). An institutional review board approval was obtained.

Table 1. Characteristics of treatment planning and irradiation targets.

Characteristic		Total (n = 24)
Prescription/fraction	27 Gy/3 fr	14
	30 Gy/3 fr	5
	30 Gy/5 fr	4
	33 Gy/3 fr	1
Delivered monitor unit/fraction	median (range)	2707 (1937 - 6387)
Normalization	D95%	7
	D99.5%	17
MLC margin	0 mm	11
	1 mm	13
Arc number	median (range)	10 (5 - 10)
Irradiation targets	2	5
	3	9
	4	4
	5	3
	6	3
PTV size (cm^3)	mean ± SD	1.72 ± 2.21

Abbreviations: Dx%, dose administered to x% of volume.

2.2. Treatment Planning

The radiation oncologist created all treatment plans using the Elements Multiple Brain Mets SRS (BrainLab, Munich, Germany) for a SIMT dynamic conformal arc plan (DCAT). The beam gantry angle, collimator angle, couch angle, and IC position were all calculated automatically using the target location and geometry. A Monte Carlo calculation algorithm was used, with a calculation dose grid size (GS) of 1 mm. The Monte Carlo spatial resolution was set to 2.3 mm × 2.3 mm × 2.0 mm. This was set based on the pixel size of 0.7810 mm and slice thickness of 1 mm. The Monte Carlo statistical uncertainty for the final forward dose calculation was set at 2%. This was chosen to balance the time taken for optimization and uncertainty, and because it is commonly used in our hospital. The Monte Carlo dose result type could be selected from Dose to water and Dose to medium, and all of them were selected as Dose to medium. The minimum output factor was 5 mm for MLC and 8 mm for Jaw. All beam energies utilized 10 MV. An example of a treatment plan is depicted in Figure 1. Prescribed doses varied by case, with normalization at D99.5% or D95% for each target (Table 1).

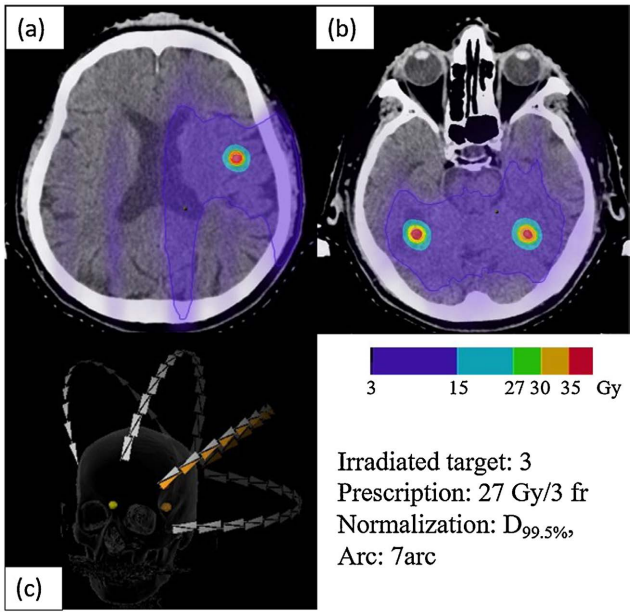

Figure 1. Treatment planning. (a) and (b) indicate the Axial dose distributions for the three targets. (c) illustrates the rotation angle of the arc. Abbreviations: D99.5%, dose administered to 99.5% of volume.

2.3. Measurement

All measurements were performed at Novalis TX (Varian Medical Systems, Palo Alto, California, USA). Two types of measurements, AC and ionization chamber, were used for all cases in this study. Three-dimensional planar gamma analysis was performed with AC as the multidimensional detector and SNC patient ver.6.7.4 (Sun Nuclear, Melbourne, FL) as the analysis software. All treatment plans included a couch angle greater than 0 degrees, but all couch angles were

measured at 0 degrees due to AC constraints. The PSQA planning doses were calculated in Monte Carlo with a non-uniformity correction. The uncertainty was 1%, and GSs of 1 mm, 1.5 mm, and 2 mm were also created, with computation times measured. Global normalization was used, and 4 different gamma criteria for dose difference (DD) / distance-to-agreement (DTA) of 3%/2 mm, 2%/2 mm, 2%/1 mm, and 1%/1 mm were used. We investigated the GPR for various parameters of GS (1.0 mm 1.5 mm and 2.0 mm), threshold (TH) (10% and 20%), and gamma analysis mode (absolute dose and relative dose). The default values were 1.0 mm for GS, 10% for threshold, and absolute dose.

The ionization chamber was a small volume chamber (TN31016 PinPoint 3D chamber, PTW, Freiburg, Germany), while the potentiometer was RAMTEC smart (TOYO MEDIC, Tokyo, Japan). An in-house head phantom (18 cm in diameter and 11 cm in length) was aligned before inserting the ionization chamber. The couch angle was identical to the actual treatment. For smaller targets, the field output correction factor (k-factor) recommended by TRS 483 [29] was used for correction. The difference between the treatment planning system (TPS) and measurements was calculated using the following equation (1).

$$\begin{aligned}&\text{Difference of isocenter dose}(\%)\\&=(\text{calculation dose}-\text{measured dose})/(\text{measured dose})\times 100\end{aligned} \tag{1}$$

2.4. Evaluation

The following three parameters were calculated from the treatment plan. The first is the "equivalent MLC field size," which is calculated by Equation (2) using the tumor radius and MLC margin.

$$\begin{aligned}&\text{Equivalent MLC field size } (mm)\\&=\sqrt{\left((\text{tumor radius}(mm)+\text{MLC margin}(mm))^2\times\pi\right)}\end{aligned} \tag{2}$$

The second is "max target IC distance," which is defined as the maximum distance between the IC and the target. The third is the "modulation factor," which is the ratio of total planned MU to the prescribed dose per fraction. Furthermore, we examined the number of detectors used for evaluation (evaluated detectors) from actual measurements of the multi-dimensional detector, *i.e.* the number of detectors that contained a dose above the threshold. Nonparametric Wilcoxon matched pair tests were performed in MATLAB R2023a (MathWorks, Natick, MA, USA) for each gamma criterion in each group. Due to the sample size, all nonparametric Wilcoxon signed-rank tests were used to assess significant differences without regard for whether they followed a normal distribution. p-values < 0.05 were deemed statistically significant. The default GPR was investigated using four parameters: equivalent MLC field size, max target-IC distance, modulation factor, and max differences of the chamber. Furthermore, because all treatment plans were generated by DCAT, the modulation factor was assumed to depend on the number, size, and location of the targets. Thus, the relationship between

"equivalent MLC field size (minimum and average)" and "modulation factor" was investigated. Multiple regression analysis was performed to identify the independent contribution of each parameter to GPR. This used GPR as the objective variable and the five parameters (number of targets, minimum target volume, max target-IC distance, and number of evaluated detectors) as the explanatory variables.

3. Results

Figure 2 displays the GPRs for the four criteria. In the 3%/2 mm criterion, increasing GS from 1 mm (default) to 1.5 mm and 2 mm reduced mean GPR by 2.9% and 5.3%, respectively. Similarly, in the other criteria, changing the GS resulted in a decrease in GPR, with the decrease being greater in the more severe criteria. There were no significant differences between the different GSs in any of the criteria. (GS1.5 mm: 3%/2 mm, 2%/2 mm, 2%/1 mm, and 1%/1 mm were p = 0.31, 0.38, 0.39, and 0.36, respectively) (GS2.0 mm: 3%/2 mm, 2%/2 mm, 2%/1 mm, and 1%/1 mm were p = 0.08, 0.10, 0.08, and 0.07, respectively). For the calculation times shown in Table 2(a), GS1.5 mm and GS2.0 mm were 245 s (67%) and 290 s (79%) faster than GS1.0 mm.

For the number of evaluated detectors shown in Table 2(b), increasing the TH from 10% to 20% resulted in an average of 154 fewer detectors being evaluated,

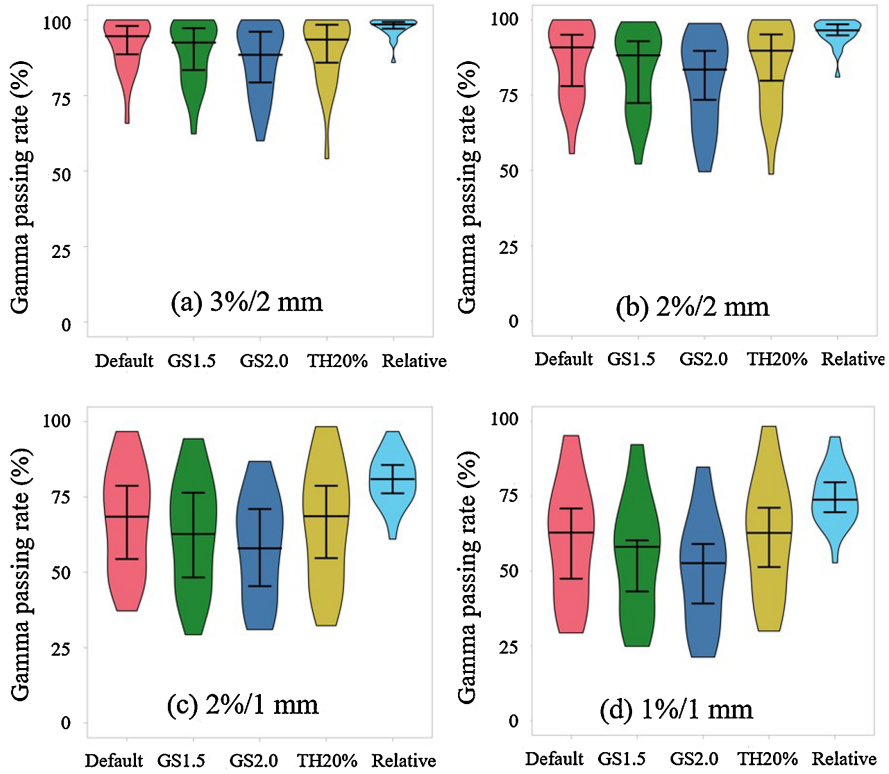

"Default" is 1.0 mm for grid size, 10% for threshold, and absolute dose. "Relative" was evaluated as a relative dose. There were notable differences only between "Default" and "Relative" in all criteria.

Figure 2. All criteria of gamma passing ratio.

Table 2. (a) Calculation time of QA planning. (b) Number of evaluated detectors.

(a)		
	Mean (sec)	Range (sec)
GS 1.0 mm	363	115 - 563
GS 1.5 mm	118	50 - 197
GS 2.0 mm	73	31 - 127
(b)		
	Mean	Range
AD, TH10%	540	281 - 814
AD, TH20%	386	216 - 602
RD, TH10%	596	319 - 852

Abbreviations: GS, grid size; AD, absolute dose; RD, relative dose; TH, threshold.

but there were no significant differences in pass rates across all criteria (3%/2 mm, 2%/2 mm, 2%/1 mm, and 1%/1 mm were p = 0.43, 0.69, 0.80, and 0.74 for, respectively).

When comparing absolute and relative dose dosimetry, the mean GPR was higher for relative dose in all criteria, and the variation in GPR was smaller. Only the relative dose differed significantly from the absolute dose in all criteria (3%/2 mm, 2%/2 mm, 2%/1 mm, and 1%/1 mm were p = 0.0056, 0.0013, 0.0023, and 0.0017 for, respectively). In all cases, relative dosimetry had a greater number of active detectors, approximately 54 more on average (**Table 2(b)**).

The effect of DD or DTA on the GPR was investigated by examining the default mean GPR based on various criterion. When comparing **Figure 2(a)** 3%/2 mm and (b) 2%/2 mm, the GPR decreased from 91.8% to 86.4% for the same DTA criteria (p = 0.091). Similarly, when comparing **Figure 2(c)** 2%/1 mm and (d) 1%/1 mm, GPR fell from 67.8% to 60.2% (p = 0.158). In contrast, comparing **Figure 2(b)** 2%/2 mm and **Figure 2(c)** 2%/1 mm with different DTA, the GPR decreased relatively significantly (18.6%) from 86.4% to 67.8% (p < 0.001).

Figure 3 depicts the relationship between the four parameters and the GPR. The relationship between equivalent MLC field size and GPR is depicted in **Figure 3(a-1)** and **Figure 3(a-2)**. The median of minimum and average equivalent MLC field sizes were 9.5 mm and 12.7 mm, respectively. **Figure 3(a-1)** demonstrates that the GPR decreases when the minimum equivalent MLC field size of multiple targets is small, particularly when it is less than 10 mm (R^2 = 0.498). **Figure 3(a-2)** depicts the relationship between the average equivalent MLC field size and GPR for each plan. The average equivalent MLC field size showed a stronger correlation than the minimum equivalent MLC field size (R^2 = 0.596).

Figure 3(b) depicts the relationship between the max dose difference in the chamber and GPR. The higher the max dose difference in the chamber, the lower the GPR (R^2 = 0.282).

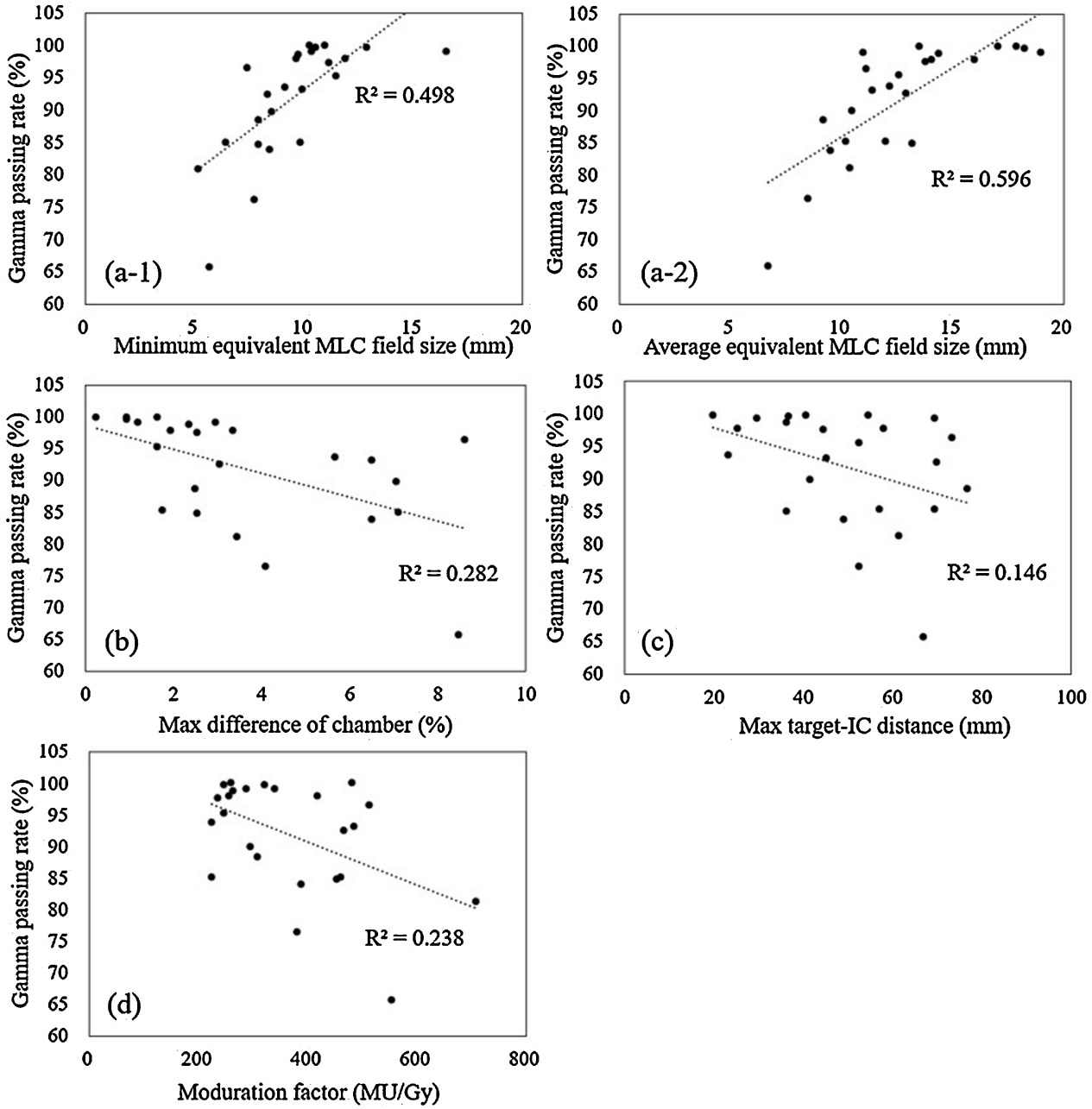

Figure 3. Correlation between the four parameters and gamma passing rate.

Figure 3(c) depicts the relationship between the max target-IC distance and GPR, which shows a low correlation ($R^2 = 0.146$).

Figure 3(d) shows that the GPR decreased slightly as the modulation factor increased ($R^2 = 0.238$).

Figure 4(a) depicts the relationship between the minimum equivalent MLC field size and the max dose difference of isocenter dose. In all treatment plans, the chamber's max dose difference was the target with the smallest equivalent MLC field size among all targets. As with GPR, the max dose difference of isocenter dose increased when the equivalent MLC field size was less than 10 mm ($R^2 = 0.380$).

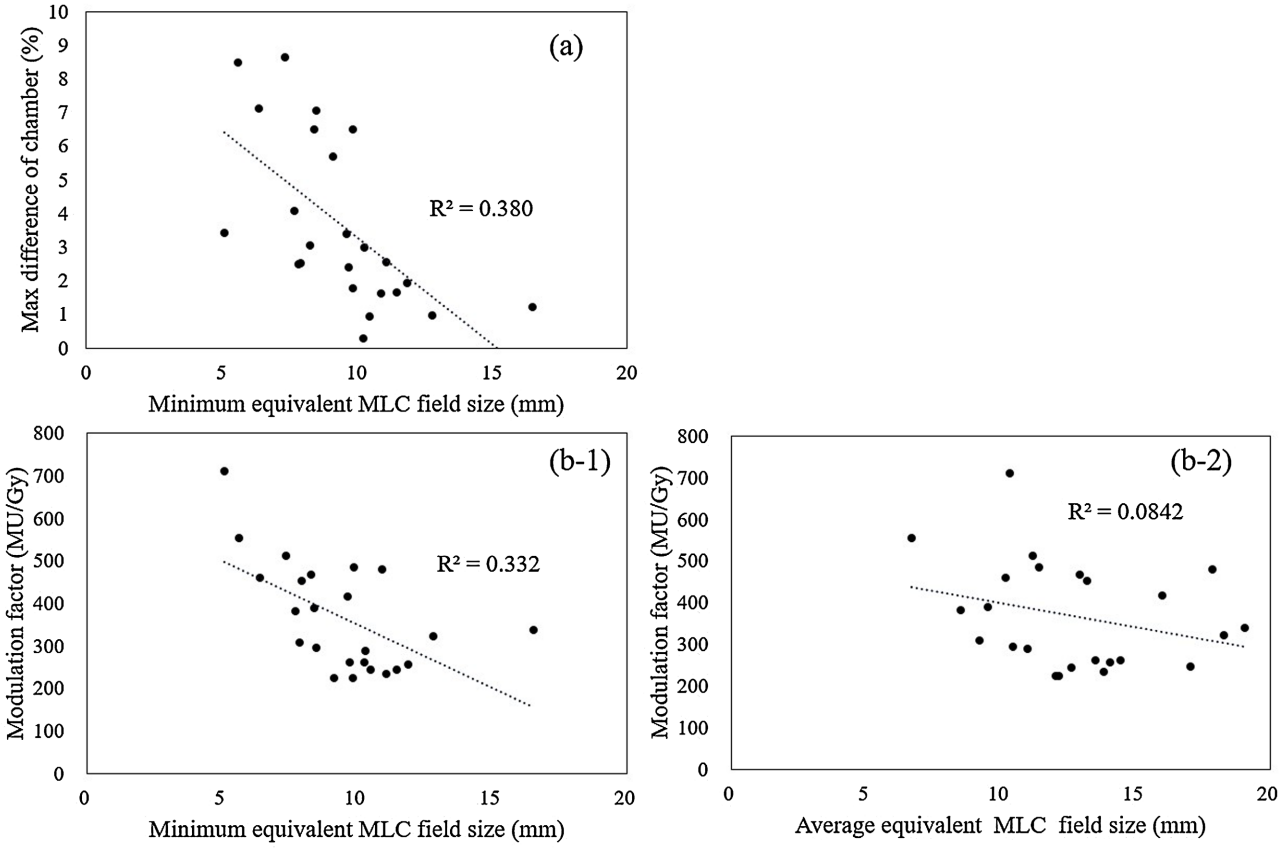

Figure 4. Relationship between two indicators and equivalent MLC field size.

The relationship between "equivalent MLC field size (minimum and average)" and "modulation factor" is illustrated in **Figure 4(b-1)** and **Figure 4(b-2)**. The modulation factor correlated more strongly with the minimum equivalent MLC field size than with the average equivalent MLC field size. (R^2 = 0.332 and R^2 = 0.084 for the minimum and average, respectively).

Figure 5 depicts the dose distribution as measured with an actual multidimensional detector. **Figure 5(b)-(d)** focus on the b, c, and e cross sections of the distribution in (a), respectively, with the detector measurements on the vertical axis and the detector location on the horizontal axis. **Figure 5(b)** and **Figure 5(d)** show a good agreement between the TPS and measured doses in the target's central region. On the other hand, the left side of **Figure 5(c)** depicts a slightly off-center part of the target with measured values that are generally lower than those of the TPS and a point of failure.

When multiple regression analysis was performed with GPR as the dependent variable, the coefficient of determination (R^2) was 0.851, and the adjusted coefficient of determination (Adj. R^2) was 0.786. The F-value was 13.05, and the p-value was 1.51e−05, so the model as a whole was statistically significant. The significant positive influence was the number of evaluated detectors, with a regression coefficient of 0.1179 and a p-value of 0.001. The p-value for minimum target volume was 0.093, which was not statistically significant, but the regression coefficient

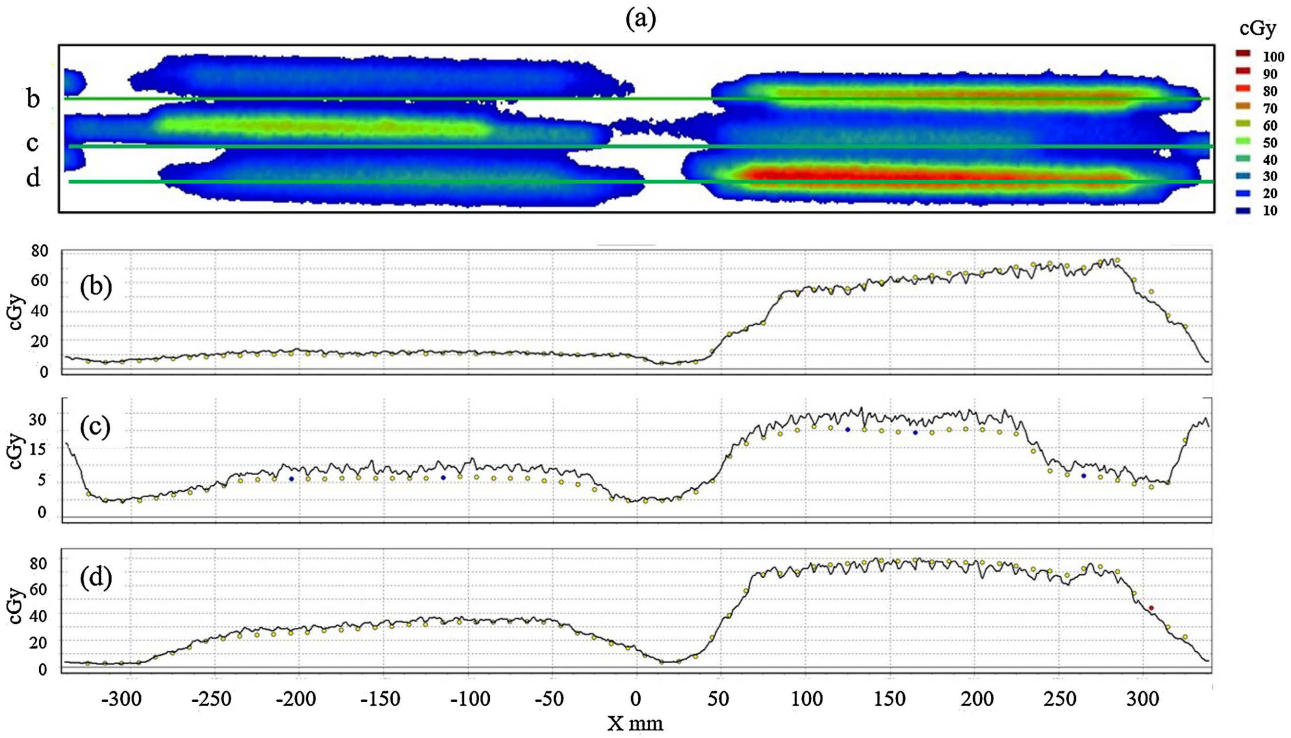

Figure 5. Dose distribution of ArcCHECK. (b), (c), and (d) focus on the b, c, and e cross sections of the distribution in (a), respectively, with the detector measurements on the vertical axis and the detector location on the horizontal axis. Solid lines indicate TPS, and ○ represents the measured values of each detector. The points that passed at 3% 2 mm of criterion are depicted in yellow, and the points that failed are indicated in blue.

was 0.8566. There was no significant difference for the other variables.

4. Discussion

This study investigated the relationship between GPR and treatment plan-dependent parameters such as PTV size and distance from the isocenter in patient QA using ArcCHECK in SIMT.

It reported that in previous studies, a smaller GS (1.0 mm) results in a higher GPR, which is consistent with our findings [30]. AAPM TG 101 recommends a GS of 2 mm or less for SBRT [31] while Medical Physics Practice guideline 9.a. states that a 1 mm GS in the TPS calculation may be required for very small targets [10]. The multiple brain metastases in this study were small targets, with a median target volume of 0.8 cm^3 and a median diameter of 1.16 cm when assumed to be a sphere. Therefore, a smaller GS enabled more accurate dose calculation, demonstrating the utility of a smaller GS. The smaller the GS, the longer the calculation time, but even at the maximum, it was within 10 minutes, so if it is within an acceptable range, a GS of 1.0 mm or less is recommended.

Different TH (10% and 20%) and dose evaluation (relative and absolute dose) varied the number of active detectors. Increasing the TH from 10% to 20% was considered so that the evaluation could focus on the higher dose range. The dif-

ference in TH reduced the number of active detectors by an average of 154; however, there was no significant difference in GPR results. If the TH had been higher, the outcomes might have been different. In comparison to the absolute dose mode, the relative dose mode had more active detectors (**Table 2(b)**), and a higher GPR. This is because the relative dose adjusts the dose so that the GPR is maximized, and in many cases, the measured dose is lower than planned due to the wide detector spacing, so the analysis shifts to increase the dose. However, in the event of a dose error, the relative dose mode may underestimate the error, so the absolute dose, as recommended by the guideline, is preferred [32].

We investigated the effect of the criteria DD or DTA on the GPR. When DTA was 1 mm tighter, the GPR decreased significantly. Specifically, in **Table 3**, GPR decreased from 86.4% at 2% 2 mm to 67.9% at 2% 1 mm, an average decrease of 18.6%. On the other hand, stricter DD criteria resulted in a lower GPR, but not a noticeable decrease. In **Table 3**, GPR decreased by an average of only 5.4%, from 91.8% at 3% 2 mm to 86.4% at 2% 2 mm. Therefore, when compared to DD, DTA was found to be significantly related to the GPR, possibly due to the small size of the SIMT SRT target, steep dose gradient, and misalignment of the ACs, all of which directly resulted in a lower GPR. Lee *et al.* also found that changing the GPR from 3%/2 mm to 2%/2 mm reduced the average GPR by 2.20% while changing from 2%/2 mm to 2%/1 mm decreased the average pass rate by 11.21% [30]. They also noted that meeting the DTA standard of 1 mm appears to be difficult even for homogeneous plans like DCAT, and their findings were consistent with those in this study. It can be said that this study has provided a guide to the GPR for each criterion when using ArcCHECK as a multi-dimensional detector.

Table 3 presents a comparison of previous studies. Although different studies used different criteria, all performed gamma analysis in global mode with a TH of 10%. Because they were limited to SRT cases, studies with a single target were included. The average GPR for a single target exceeded 90%, even with the stringent criterion (2mm/1%) (**Table 3** (b) [32], (c) [30], and (d) [30]). However, using the 2%/1 mm criterion, the mean GPR of our results was significantly lower than that of all three previous studies (**Table 3** (a) [32], (e) [33], and (f) [11]). **Table 3(e)** shows that only 11 of the 40 plan samples were intracranial, and many of them had relatively large targets (target volume sizes ranged from 0.43 cm^3 to 161.13 cm^3, with a mean volume of 35.81 cm^3). For **Table 3(f)**, absolute dose calibration was performed on the measurement day, and the setup was done by MV imaging devices. In our study, we obtained the absolute dose calibration annually, and we trust our laser in setting up AC. Therefore, we assume that these differences in settings influenced the GPR. For **Table 3(a)**, the difference in arc number may have influenced the results. Although VMAT had more modulation than DCAT, the median number of arcs was less than half (4.3 vs. 10). It is difficult to make a simple comparison because the low-dose range expands when fewer MUs are irradiated with more arcs. Namely, as illustrated in **Figure 5(c)**, there were numerous areas where the measured doses were lower than calculated doses at

low doses. This could explain why irradiation in DCAT resulted in lower GPR than in VMAT.

Table 3. Characteristics of treatment planning and irradiation targets.

Study	Our study	(a) Xia *et al* [32]	(b) Xia *et al* [32]	(c) Lee *et al* [30]	(d) Lee *et al* [30]	(e) James *et al* [33]	(f) Dunn *et al* [11]
Year		2020	2020	2021	2021	2023	2024
4%/1 mm	-	98.64	99.14	-	-	-	-
3%/3 mm	-	99.74	99.76	99.96	99.42	96.43	100.0
3%/2 mm	91.81	99.47	99.56	99.88	98.60	-	-
3%/1 mm	-	97.50	97.20	-	-	-	-
2%/2 mm	86.41	-	-	99.79	98.00	90.20	-
2%/1 mm	67.85	94.16	94.04	96.44	90.64	79.52	100.0
1%/1 mm	60.18	-	-	-	-	69.20	100.0
Irradiation method	DCAT	VMAT	VMAT	DCAT	VMAT	IMRT, VMAT	VMAT
Number of treatment planning	24	49	25	20	8	40 (11 cranial)	1
Number of targets	Multi	Multi	Single	Single	Single	Multi	Multi (21)

Gamma analysis was conducted in Global mode and a threshold of 10% was employed for all studies.

Figure 5 shows that TPS and measured values tended to agree at the detector rows that received a direct beam. However, the measured values were lower than the TPS at the beam's edge (low-dose area), which is slightly further away from the target, and this area contributed to the decrease in GPR in many cases. Figure 3(a-1) shows that the GPR decreases when the minimum equivalent MLC field size is less than 10 mm. This is also probably due to detector spacing. The multi-dimensional detector used in this study had a detector spacing of 10 mm, which may have resulted in an underestimated dose. Figure 3(b) shows that the max dose difference of isocenter dose also tends to increase when the equivalent MLC field size is less than 10 mm, like the GPR. This could be because the correction for small irradiation fields, known as k-factor, factors that add up to an irradiation field of less than 10 mm, is not recommended. Therefore, both the ionization chamber and the multidimensional detector may underestimate the dose when the equivalent MLC field size is below 10 mm. As depicted in Figure 3(a-1) and Figure 3(a-2), it was more related to average size than minimum size. This could be because many of the targets were small to begin with, making average, a measure of the sum of multiple targets, more relevant. The GPR tends to decrease as the modulation factor increases. In particular, while not as large as the average equivalent MLC field size, the modulation coefficient is related to the minimum equivalent MLC field size, so we believe there was a correlation. Prabhakar *et al*

found a strong correlation of $R^2 = 0.97$ between the equivalent square field size (the standard 4 * Area/Perimeter) of the IMRT plan and the GPR of 3%/2 mm, indicating that GPR depends on the field size [34]. DCAT produced similar results, despite using a different field size calculation method.

However, there was little correlation between max target-IC distance and GPR (**Figure 3(d)**). Although we could not find any reports on the relationship between GPR and target-IC distance, we hypothesized based on the two reports that GPR may decrease as target-IC distance increases (ExacTrac-based alignment has an error of up to 2.2 mm at distances greater than 10 cm between target-IC concerning spatial accuracy [14]. Target-IC distance influences target coverage, with smaller targets having a larger effect [35].) However, in this study, we could not accurately investigate the relationship between target-IC distance and GPR, including the effect of rotation, because all measurements were taken with the couch set to 0˚. Therefore, it is possible that the target-IC distance has less of an effect on GPR and that the effect has been reduced because the couches have not been rotated.

Multiple regression analysis showed that the GPR at 2% 2 mm was greater when there were more detectors (number of evaluated detectors) that detected a dose of 10% or more of the prescribed dose. The number of evaluated detectors is thought to increase when the targets are far apart or the targets are large (The correlation coefficient between the number of evaluated detectors and the maximum distance between the target ICs was 0.60, and the correlation coefficient with the number of targets was 0.54, indicating a moderate correlation.). Previous research has also stated that larger targets result in higher GPR. On the other hand, it is generally thought that the further apart the targets are, the greater the likelihood of a larger error, but with the number of evaluated detectors increasing, the GPR tends to be larger in the AC than when the targets are close to each other. This is likely to be a phenomenon unique to the AC. In other words, when the targets are small and close to each other, the number of detectors that evaluate them decreases, and the impact of the detectors that fail increases, so even if there are no problems with the treatment plan, the GPR may decrease.

There are some limitations to this study. The first is that the evaluation does not consider error detection sensitivity. Several previous studies have reported that AC does not have high sensitivity to gantry and collimator rotation errors, as well as MLC positioning errors. For example, Liang *et al.* reported that the minimum reliably detectable gantry rotation and MLC leaf positioning errors were 2˚ and 4 mm, respectively [36]. Leon *et al.* found that MLC positioning errors were consistently undetectable [11]. Tutty *et al.* found that the AC could detect introduced errors in the delivery of treatment plans with large target volumes of about 3 cm using the 3%/1 mm gamma criterion, but was insensitive to introduced errors in treatment plans with smaller target volumes of about 1.5 cm [37]. In contrast, it is more sensitive to setup errors in couch translation and rotation. The 2%/2 mm gamma criterion results in a 6.7% ± 3.5% and 14.5% ± 6.6% reduction

in GPR for 2 mm translation and 2° rotation errors, respectively [38]. AC error detection limits should be considered when performing PSQA. Second, measuring was impossible with the couch rotated. AAPM TG 218 recommends the true composite (TC) method. This is because the TC method is preferred for PSQA of SRS and SBRT treatments, in which the measurement device is placed on the couch with actual treatment parameters such as gantry, collimator, couch angle, jaws, MLC leaf position, MU, and the radiation beam is delivered to simulate treatment delivery to the patient [39]. The findings and conclusions in this study may be inaccurate when compared to the results of PSQA obtained using the TC method. More specifically, the results are likely to be worse if the couch's residual rotational error is considered.

AC has been linked to several negative outcomes. Low spatial resolution causes a sharp drop in GPR when the criteria are tightened. The response is low due to the low dose at detectors located outside the direct beam area. In other words, the detector array's configuration and resolution significantly affect the experimental calculation of gamma due to under sampling of the dose distribution, blurring effects, noise, or a combination of both. However, it is unaffected by volume averaging, unlike ionization chambers. The measurement is nearly independent of target size and positional relationship, and it can be completed in a single step. This saves a significant amount of physics QA time. In high-volume radiotherapy facilities, it can improve physics throughput while reducing human error. After the text edit has been completed, the paper is ready for the template. Duplicate the template file by using the Save As command, and use the naming convention prescribed by your journal for the name of your paper. In this newly created file, highlight all of the contents and import your prepared text file. You are now ready to style your paper.

5. Conclusion

This study used AC to investigate the relationship between target- and treatment plan-dependent parameters and the GPR to determine the utility and caution in using PSQA with AC in SIMT. Because the average equivalent MLC field size is moderately correlated with the GPR, it was clear that the GPR drops significantly when the target is small, particularly below 10 mm.

Acknowledgments

The authors have nothing to report.

Conflicts of Interest

The authors declare no conflicts of interest regarding the publication of this paper.

References

[1] Brown, P.D., Jaeckle, K., Ballman, K.V., Farace, E., Cerhan, J.H., Anderson, S.K., *et al.* (2016) Effect of Radiosurgery Alone vs Radiosurgery with Whole Brain Radiation

Therapy on Cognitive Function in Patients with 1 to 3 Brain Metastases: A Randomized Clinical Trial. *JAMA*, **316**, 401-409. https://doi.org/10.1001/jama.2016.9839

[2] Palmer, J.D., Sebastian, N.T., Chu, J., DiCostanzo, D., Bell, E.H., Grecula, J., *et al.* (2020) Single-Isocenter Multitarget Stereotactic Radiosurgery Is Safe and Effective in the Treatment of Multiple Brain Metastases. *Advances in Radiation Oncology*, **5**, 70-76. https://doi.org/10.1016/j.adro.2019.08.013

[3] Yamamoto, M., Serizawa, T., Higuchi, Y., Sato, Y., Kawagishi, J., Yamanaka, K., *et al.* (2017) A Multi-Institutional Prospective Observational Study of Stereotactic Radiosurgery for Patients with Multiple Brain Metastases (JLGK0901 Study Update): Irradiation-Related Complications and Long-Term Maintenance of Mini-Mental State Examination Scores. *International Journal of Radiation Oncology·Biology·Physics*, **99**, 31-40. https://doi.org/10.1016/j.ijrobp.2017.04.037

[4] Clark, G.M., Popple, R.A., Young, P.E. and Fiveash, J.B. (2010) Feasibility of Single-Isocenter Volumetric Modulated Arc Radiosurgery for Treatment of Multiple Brain Metastases. *International Journal of Radiation Oncology·Biology·Physics*, **76**, 296-302. https://doi.org/10.1016/j.ijrobp.2009.05.029

[5] Roper, J., Chanyavanich, V., Betzel, G., Switchenko, J. and Dhabaan, A. (2015) Single-Isocenter Multiple-Target Stereotactic Radiosurgery: Risk of Compromised Coverage. *International Journal of Radiation Oncology·Biology·Physics*, **93**, 540-546. https://doi.org/10.1016/j.ijrobp.2015.07.2262

[6] Stanhope, C., Chang, Z., Wang, Z., Yin, F., Kim, G., Salama, J.K., *et al.* (2016) Physics Considerations for Single-Isocenter, Volumetric Modulated Arc Radiosurgery for Treatment of Multiple Intracranial Targets. *Practical Radiation Oncology*, **6**, 207-213. https://doi.org/10.1016/j.prro.2015.10.010

[7] Feygelman, V., Walker, L., Chinnaiyan, P. and Forster, K. (2008) Simulation of Intrafraction Motion and Overall Geometric Accuracy of a Frameless Intracranial Radiosurgery Process. *Journal of Applied Clinical Medical Physics*, **9**, 68-86. https://doi.org/10.1120/jacmp.v9i4.2828

[8] Saglam, Y., Bolukbasi, Y., Atasoy, A.I., Karakose, F., Alpan, V., Selek, U., *et al.* (2020) Quality Assurance in Stereotactic Radiosurgery and Stereotactic Body Radiotherapy. *Advances in Research*, **21**, 22-33. https://doi.org/10.9734/air/2020/v21i730216

[9] Benedict, S.H., Cai, J., Libby, B., Lovelock, M., Schlesinger, D., Sheng, K., *et al.* (2010) SRT and SBRT: Current Practices for QA Dosimetry and 3D. *Journal of Physics: Conference Series*, **250**, Article 012057. https://doi.org/10.1088/1742-6596/250/1/012057

[10] Halvorsen, P.H., Cirino, E., Das, I.J., Garrett, J.A., Yang, J., Yin, F., *et al.* (2017) AAPM-RSS Medical Physics Practice Guideline 9.a. for SRS-SBRT. *Journal of Applied Clinical Medical Physics*, **18**, 10-21. https://doi.org/10.1002/acm2.12146

[11] Dunn, L., Tamborriello, A., Subramanian, B., Xu, X. and Ruruku, T.T. (2024) Assessing the Sensitivity and Suitability of a Range of Detectors for SIMT PSQA. *Journal of Applied Clinical Medical Physics*, **25**, e14343. https://doi.org/10.1002/acm2.14343

[12] Farhood, B., Parwaie, W., Refahi, S. and Ardekani, M. (2018) Different Dosimeters/Detectors Used in Small-Field Dosimetry: Pros and Cons. *Journal of Medical Signals & Sensors*, **8**, 195-203. https://doi.org/10.4103/jmss.jmss_3_18

[13] Pappas, E., Maris, T.G., Zacharopoulou, F., Papadakis, A., Manolopoulos, S., Green, S., *et al.* (2008) Small SRS Photon Field Profile Dosimetry Performed Using a Pinpoint Air Ion Chamber, a Diamond Detector, a Novel Silicon-Diode Array (DOSI), and Polymer Gel Dosimetry. Analysis and Intercomparison. *Medical Physics*, **35**, 4640-4648.

https://doi.org/10.1118/1.2977829

[14] Ezzell, G.A. (2017) The Spatial Accuracy of Two Frameless, Linear Accelerator-Based Systems for Single-Isocenter, Multitarget Cranial Radiosurgery. *Journal of Applied Clinical Medical Physics*, **18**, 37-43. https://doi.org/10.1002/acm2.12044

[15] Cullom, E.T., Xia, Y., Chuang, K., Gude, Z.W., Zlateva, Y., Adamson, J.D., *et al.* (2021) Single Isocenter SRS Using CAVMAT Offers Improved Robustness to Commissioning and Treatment Delivery Uncertainty Compared to Vmat. *Journal of Applied Clinical Medical Physics*, **22**, 36-43. https://doi.org/10.1002/acm2.13248

[16] Goodall, S.K., Dunn, L., Dunning, J., Muñoz, L., Rowshanfarzad, P. and Ebert, M.A. (2022) Matched Linac Stereotactic Radiotherapy: An Assessment of Delivery Similarity and Distributive Patient-Specific Quality Assurance Feasibility. *Journal of Applied Clinical Medical Physics*, **23**, e13652. https://doi.org/10.1002/acm2.13652

[17] Salari, E., Parsai, E.I., Shvydka, D. and Sperling, N.N. (2021) Evaluation of Parameters Affecting Gamma Passing Rate in Patient-Specific Qas for Multiple Brain Lesions IMRS Treatments Using Ray-Station Treatment Planning System. *Journal of Applied Clinical Medical Physics*, **23**, e13467. https://doi.org/10.1002/acm2.13467

[18] Chang, J., Wernicke, G. and Pannullo, S.C. (2018). Restricted Single Isocenter for Multiple Targets Dynamic Conformal Arc (RSIMT DCA) Technique for Brain Stereotactic Radiosurgery (SRS) Planning. *Journal of Radiosurgery and SBRT*, **5**, 145-156. https://pmc.ncbi.nlm.nih.gov/articles/PMC5893455/

[19] McCulloch, J., Pawlowski, J., Kirby, N., Rasmussen, K., Shi, Z., Myers, P., *et al.* (2020) Patient-Specific Dose Quality Assurance of Single-Isocenter Multiple Brain Metastasis Stereotactic Radiosurgery Using PTW Octavius 4D. *Journal of Applied Clinical Medical Physics*, **21**, 107-115. https://doi.org/10.1002/acm2.12979

[20] Junis, I., Yousif, Y., Stensmyr, R. and Barber, J. (2024) Comprehensive Characterisation of the IBA Myqa SRS for SRS and SBRT Patient Specific Quality Assurance. *Physical and Engineering Sciences in Medicine*, **47**, 327-337. https://doi.org/10.1007/s13246-023-01370-0

[21] Knill, C., Sandhu, R., Halford, R., Snyder, M. and Seymour, Z. (2021) Commissioning Cranial Single-Isocenter Multi-Target Radiosurgery for the Versa Hd. *Journal of Applied Clinical Medical Physics*, **22**, 108-114. https://doi.org/10.1002/acm2.13223

[22] Hoopingarner, S., Oldham, M., Adamson, J. and Lakrad, K. (2023) Investigation of a 3D Dosimetry System Utilizing Radio-Chromic Gel and Telecentric Optical-CT Readout. *Medical Physics*, **50**, 5734-5744. https://doi.org/10.1002/mp.16632

[23] Calvo-Ortega, J., Greer, P.B., Moragues-Femenía, S., Pozo-Massó, M. and Casals-Farran, J. (2022) Verification of Stereotactic Radiosurgery Plans for Multiple Brain Metastases Using a Virtual Phantom-Based Procedure. *Reports of Practical Oncology and Radiotherapy*, **27**, 449-457. https://doi.org/10.5603/rpor.a2022.0042

[24] Dunn, L. and Jolly, D. (2018) Automated Data Mining of a Plan-Check Database and Example Application. *Journal of Applied Clinical Medical Physics*, **19**, 739-748. https://doi.org/10.1002/acm2.12396

[25] Jolly, D., Dunn, L. and Kenny, J. (2016) A Clinical Database to Assess Action Levels and Tolerances for the Ongoing Use of Mobius3D. *Journal of Applied Clinical Medical Physics*, **18**, 59-65. https://doi.org/10.1002/acm2.12009

[26] Han, Z., Hacker, F., Killoran, J., Kukluk, J., Aizer, A. and Zygmanski, P. (2019) Optimization of MLC Parameters for TPS Calculation and Dosimetric Verification: Application to Single Isocenter Radiosurgery of Multiple Brain Lesions Using Vmat. *Biomedical Physics & Engineering Express*, **6**, Article 015004.

https://doi.org/10.1088/2057-1976/ab57ce

[27] Adamson, J., Erickson, B.G., Wang, C., Cui, Y., Alber, M., Kirkpatrick, J., *et al.* (2023) Generation, Validation, and Benchmarking of a Commercial Independent Monte Carlo Calculation Beam Model for Multi-Target SRS. *Zeitschrift für Medizinische Physik*. https://doi.org/10.1016/j.zemedi.2023.08.004

[28] Erickson, B., Cui, Y., Alber, M., Wang, C., Fang Yin, F., Kirkpatrick, J., *et al.* (2024) Independent Monte Carlo Dose Calculation Identifies Single Isocenter Multi-Target Radiosurgery Targets Most Likely to Fail Pre-Treatment Measurement. *Journal of Applied Clinical Medical Physics*, **25**, e14290. https://doi.org/10.1002/acm2.14290

[29] Palmans, H., Andreo, P., Huq, M.S., Seuntjens, J., Christaki, K.E. and Meghzifene, A. (2018) Dosimetry of Small Static Fields Used in External Photon Beam Radiotherapy: Summary of TRS-483, the IAEA-AAPM International Code of Practice for Reference and Relative Dose Determination. *Medical Physics*, **45**, e1123-e1145. https://doi.org/10.1002/mp.13208

[30] Lee, Y. C., & Kim, Y. (2021). A Patient-Specific QA Comparison between 2D and 3D Diode Arrays for Single-Lesion SRS and SBRT Treatments. *Journal of Radiosurgery and SBRT*, **7**, 295-307. https://pmc.ncbi.nlm.nih.gov/articles/PMC8492049/

[31] Benedict, S.H., Yenice, K.M., Followill, D., Galvin, J.M., Hinson, W., Kavanagh, B., *et al.* (2010) Stereotactic Body Radiation Therapy: The Report of AAPM Task Group 101. *Medical Physics*, **37**, 4078-4101. https://doi.org/10.1118/1.3438081

[32] Xia, Y., Adamson, J., Zlateva, Y., & Giles, W. (2020). Application of TG-218 Action Limits to SRS and SBRT Pre-Treatment Patient Specific QA. *Journal of Radiosurgery and SBRT*, **7**, 135-147. https://pmc.ncbi.nlm.nih.gov/articles/PMC7717087/

[33] James, S., Al-Basheer, A., Elder, E., Huh, C., Ackerman, C., Barrett, J., *et al.* (2023) Evaluation of Commercial Devices for Patient Specific QA of Stereotactic Radiotherapy Plans. *Journal of Applied Clinical Medical Physics*, **24**, e14009. https://doi.org/10.1002/acm2.14009

[34] Ramachandran, P., Tajaldeen, A., Taylor, D., Wanigaratne, D., Roozen, K. and Geso, M. (2017) Evaluation and Performance of Arccheck and Film Using Gamma Criteria in Pre-Treatment Quality Assurance of Stereotactic Ablative Radiotherapy. *Journal of Medical Physics*, **42**, 251-257. https://doi.org/10.4103/jmp.jmp_132_16

[35] Babu, P., Selvan, K., Padma, G., Revathy, M., Nambi Raj, N. and Senthilnathan, K. (2019) Dosimetric Effect of Rotational Setup Errors in Single-Isocenter Volumetric-Modulated Arc Therapy of Multiple Brain Metastases. *Journal of Medical Physics*, **44**, 84-90. https://doi.org/10.4103/jmp.jmp_103_18

[36] Liang, B., Liu, B., Zhou, F., Yin, F. and Wu, Q. (2016) Comparisons of Volumetric Modulated Arc Therapy (VMAT) Quality Assurance (QA) Systems: Sensitivity Analysis to Machine Errors. *Radiation Oncology*, **11**, Article No. 146. https://doi.org/10.1186/s13014-016-0725-4

[37] Mark, T. (2022). Error Detection Thresholds of Diode Detector Arrays in SRT Patient Specific QA: ESTRO 2022, 6-10 May 2022, PO-1555. https://www.estro.org/Congresses/ESTRO2022/664/dosimetry/11161/errordetectionthresholdsofdiodedetectorarraysinsrt

[38] Li, G., Bai, S., Chen, N., Henderson, L., Wu, K., Xiao, J., *et al.* (2013) Evaluation of the Sensitivity of Two 3D Diode Array Dosimetry Systems to Setup Error for Quality Assurance (QA) of Volumetric-Modulated Arc Therapy (VMAT). *Journal of Applied Clinical Medical Physics*, **14**, 13-24. https://doi.org/10.1120/jacmp.v14i5.3828

[39] Miften, M., Olch, A., Mihailidis, D., Moran, J., Pawlicki, T., Molineu, A., *et al.* (2018)

Tolerance Limits and Methodologies for IMRT Measurement-Based Verification QA: *Recommendations of AAPM Task Group No.* 218. *Medical Physics*, **45**, e53-e83. https://doi.org/10.1002/mp.12810